Appl. Phys. A 75, 555–558 (2002)
DOI: 10.1007/s003390201308

Applied Physics A
Materials Science & Processing

J.E. ATWATER

Complex dielectric permittivities of the Ag_2O-Ag_2CO_3 system at microwave frequencies and temperatures between 22 °C and 189 °C

UMPQUA Research Company, P.O. Box 609, Myrtle Creek, Oregon 97 457, USA

Received: 29 October 2001/Accepted: 7 January 2002
Published online: 3 May 2002 •

ABSTRACT The silver oxide-silver carbonate system comprises a thermally regenerable chemisorbent for carbon dioxide, which has been employed to revitalize CO_2-laden air within space suits. To evaluate the compatibility of these materials with thermal regeneration via dielectric heating, complex permittivities were studied over the microwave-frequency span between 4 and 26 GHz using a vector network analyzer based measurement system. Complex permittivities were determined over temperatures from 22 °C to 189 °C. The resulting values for the real and imaginary components of the complex permittivity, corresponding to polarization and energy-loss terms, respectively, were uniformly low for both the oxide and the carbonate under all test conditions. These results suggest that efficient dielectric heating of these materials is improbable.

PACS 77.22.-d

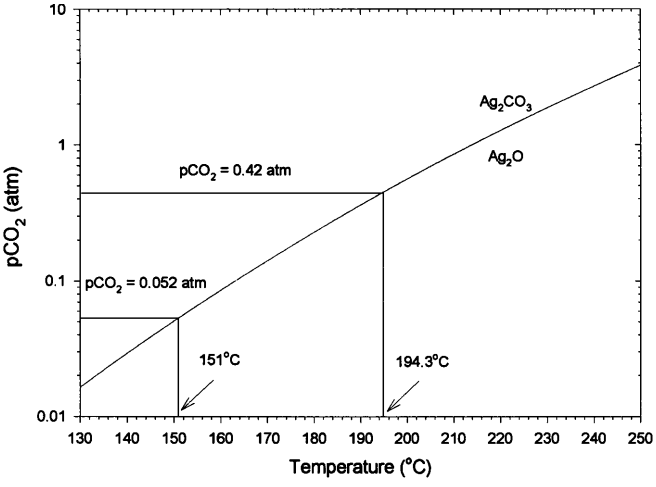

FIGURE 1 Silver carbonate-silver oxide phase diagram

1 Introduction

Silver oxide (Ag_2O) is a thermally regenerable sorbent for carbon dioxide that can be used to purify breathing air within space suits worn by astronauts during extravehicular activities (EVA) [1–3]. Carbon dioxide uptake occurs through chemisorption by silver oxide to produce silver carbonate:

$$Ag_2O_{(s)} + CO_{2(g)} \rightleftharpoons Ag_2CO_{3(s)} \,. \tag{1}$$

As shown in the phase diagram presented in Fig. 1, this reaction is thermally reversible. In comparison to other sorbents, the silver oxide-silver carbonate system imposes a relatively narrow operational temperature range for thermal regeneration. Temperatures above 160 °C are required for decomposition of the carbonate to the oxide at an appreciable rate. At temperatures above 260 °C, silver oxide rapidly decomposes to form metallic silver. Hence, means for the production of uniform and precisely regulated temperatures are required when this system is employed.

To evaluate the potential for thermal regeneration of this material via microwave (dielectric) heating, complex permittivities of silver oxide and silver carbonate were measured over a range of frequencies and temperatures. Dielectric heating through absorption of radiation at microwave frequencies involves phenomena such as induced electronic, atomic, and space-charge polarizations, or the direct coupling of electromagnetic radiation with rotational and vibrational transitions of susceptible dielectric materials to produce heat. In non-magnetic media, susceptibility to microwave heating is governed by the frequency (ω)-dependent complex permittivity [4, 5]

$$\varepsilon^*(\omega) = \varepsilon'(\omega) - \mathrm{i}\varepsilon''(\omega) \,. \tag{2}$$

The terms of ε^* are described by the Kramers–Kronig relations

$$\varepsilon'(\omega) = \varepsilon_\infty + \frac{2}{\pi}\int_0^\infty \frac{\varepsilon''(\omega)\,\omega'}{(\omega')^2 - \omega^2}\,\mathrm{d}\omega' \,, \tag{3}$$

$$\varepsilon''(\omega) = \frac{2}{\pi}\int_0^\infty \frac{\left[\varepsilon'(\omega) - \varepsilon_\infty\right]\omega}{(\omega')^2 - \omega^2}\,\mathrm{d}\omega' \,, \tag{4}$$

where ε_∞ is the permittivity at the high-frequency limit and ω' is an integration variable [6]. In the complex plane, the real and imaginary terms of $\varepsilon^*(\omega)$ correlate with polarization and

✉ Fax: +1-541/685-0339, E-mail: jatwater@engr.orst.edu

energy loss, respectively. The loss factor or dissipation factor ($\tan\delta$) is defined as

$$\tan\delta = \frac{\omega\varepsilon''(\omega)\,|\boldsymbol{E}_0|^2}{\omega\varepsilon'(\omega)\,|\boldsymbol{E}_0|^2} = \frac{\varepsilon''(\omega)}{\varepsilon'(\omega)}\,. \tag{5}$$

The average power per unit volume (P) consumed by loss mechanisms can then be calculated as

$$P = \frac{1}{2}\omega\varepsilon''\,|\boldsymbol{E}_0|^2\,. \tag{6}$$

The attenuation of a microwave beam directed along the x axis by an absorbing material is described by [7]

$$P(x) = P_0\exp(-2\alpha x)\,, \tag{7}$$

where the attenuation coefficient (α) is a function of the angular frequency (ω), the complex permittivity, and the complex permeability (μ^*):

$$\alpha = \omega\sqrt{\sqrt{\varepsilon'^2+\varepsilon''^2}\sqrt{\mu'^2+\mu''^2}} \times \sin\left[\frac{\arctan\left(\frac{\varepsilon''}{\varepsilon'}\right)+\arctan\left(\frac{\mu''}{\mu'}\right)}{2}\right]. \tag{8}$$

In non-magnetic materials, values of μ^* are extremely low; hence, microwave absorption is dominated by the complex permittivity terms. From this, it is clear that knowledge of the frequency and temperature dependences of complex permittivity in the microwave region of the electromagnetic spectrum for silver oxide and silver carbonate may be used to advantage in the modeling and design of dielectric heating systems for thermal regeneration of the chemisorbent.

2 Experimental

The complex permittivity measurement apparatus is illustrated schematically in Fig. 2. The integrated system consists of the following components: a HP8722D vector network analyzer (VNA), a HP85070B dielectric probe, a HP85056A calibration kit, and a HP85130F adapter kit. While the HP8722D VNA was capable of operation between 0.05 and 40 GHz, limitations of the dielectric probe and associated transmission elements reduced the practical working frequency range to 0.2–26 GHz. Also, dissipation ($\tan\delta$) factors ≥ 0.05 are required to assure accuracy of the test results. Complex permittivity measurements were made under software control via a Hewlett–Packard interface bus (HPIB) parallel connection between the computer and the VNA. In operation, the VNA scans a preset frequency range over which transmission and reflection parameters are determined. Material in direct contact with the dielectric probe alters the phases and magnitudes of reflected power observed by the VNA. Complex permittivities were calculated from the measured transmission and reflection parameters using HP85071B software.

To confirm the validity of complex permittivity data generated by this system, a series of aqueous 1,5-pentanediol solutions was examined at 25 °C. Four solutions were analyzed, covering the full range of pentanediol mole fractions (χ) between 0 and 1. The data acquired in our laboratory were then compared to the recently published results of Wang et al. [8], which had been derived using substantially different methods based upon a circular waveguide/interferometric technique. Polarization relaxation times and static dielectric constants calculated from the VNA-based complex permittivity data were in close agreement to the previously reported results.

To measure complex permittivities at elevated temperatures, the dielectric probe was mounted inside a gravity convection oven. To minimize temperature gradients, the oven was modified by sealing the external air convection current ports, and the addition of an internal recirculation fan. Improved temperature control was achieved using a digital PID controller and a K-type thermocouple probe mounted inside the oven. A 610-mm precision mercury thermometer covering the temperature range between −1 °C and 201 °C with 0.2 °C resolution was used to monitor the temperature of the test specimen. Both the thermocouple probe and the mercury thermometer were inserted into a sand-filled beaker of equivalent volume and elevation within the oven as the material under study. A high-temperature semi-rigid coaxial cable was used to connect the oven-mounted dielectric probe with the external VNA. Access for the thermocouple, thermometer, and coaxial cable was established through a 5.0-cm-diameter insulation-filled circular opening at the top of the oven. Temperature regulation was accurate to within ±0.2 °C.

The complex permittivities of silver oxide and silver carbonate (Aldrich, Milwaukee) were determined at five temperatures covering the approximate range between 20 and

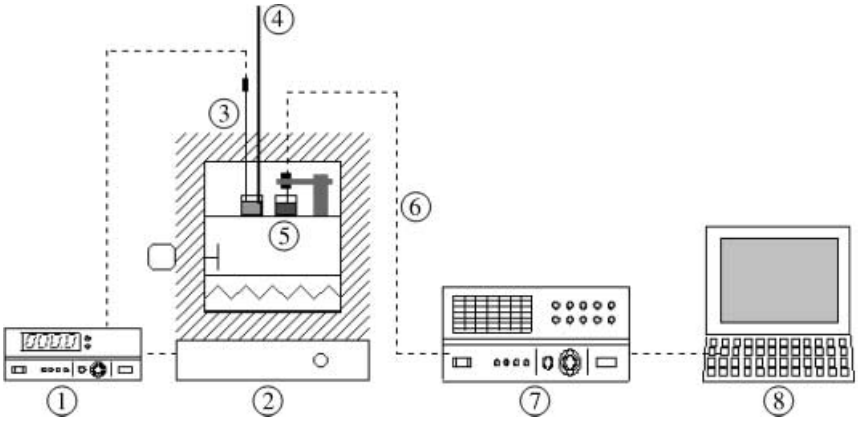

FIGURE 2 Complex permittivity test apparatus: (1) temperature controller, (2) oven, (3) thermocouple, (4) Hg thermometer, (5) dielectric probe immersed in sample, (6) high-temperature semi-rigid coaxial cable, (7) vector network analyzer, and (8) computer

200 °C. Samples were presented to the instrument as fine powders, thus obviating the need to correct for the effects of intergranular porosity. To minimize interference from adsorbed water, both materials were dried at 180 °C for a minimum of 72 h, and then stored in a desiccator prior to analysis. The instrument was first calibrated, followed by duplicate measurements at ambient temperature, with the dielectric probe in intimate contact with the material under study. The temperature was then increased. Once the set-point temperature was reached, a period of 45 min was allowed for the system to stabilize. Then a second set of duplicate measurements were made. This procedure was followed until data covering the full temperature span were gathered. The numerical values of all complex permittivities were calculated as dimensionless relative permittivities ($\varepsilon^*/\varepsilon_0$). These may be converted to absolute permittivities through multiplication by the permittivity of free space (ε_0), in appropriate units.

3 Results and discussion

The real and imaginary components of the complex permittivities for silver carbonate and silver oxide as functions of both frequency and temperature are presented in Figs. 3 and 4, respectively. Dissipation factors for these two materials are illustrated in Figs. 5 and 6. For both materials, both real and imaginary components of the complex permittivity are relatively low over the complete frequency spectrum, for all temperatures. While data were gathered across the frequency span between 0.2 and 26 GHz, the requirement of tan $\delta \geq 0.5$ for data validity was not met at the lower frequencies. Usable data resulted generally in the range between 4 and 26 GHz.

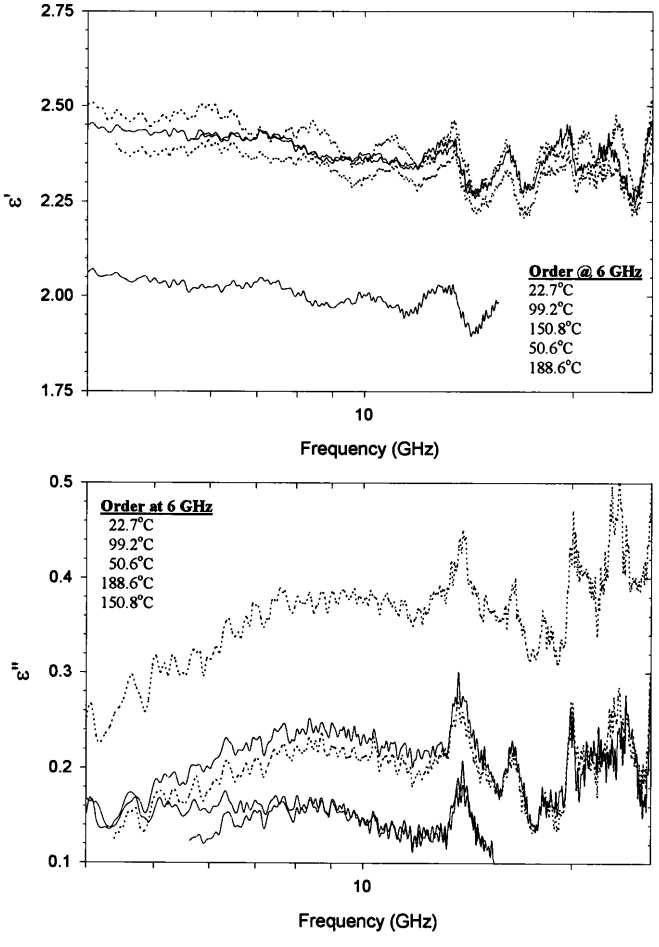

FIGURE 3 Silver carbonate: real (ε') and imaginary (ε'') components of complex permittivity

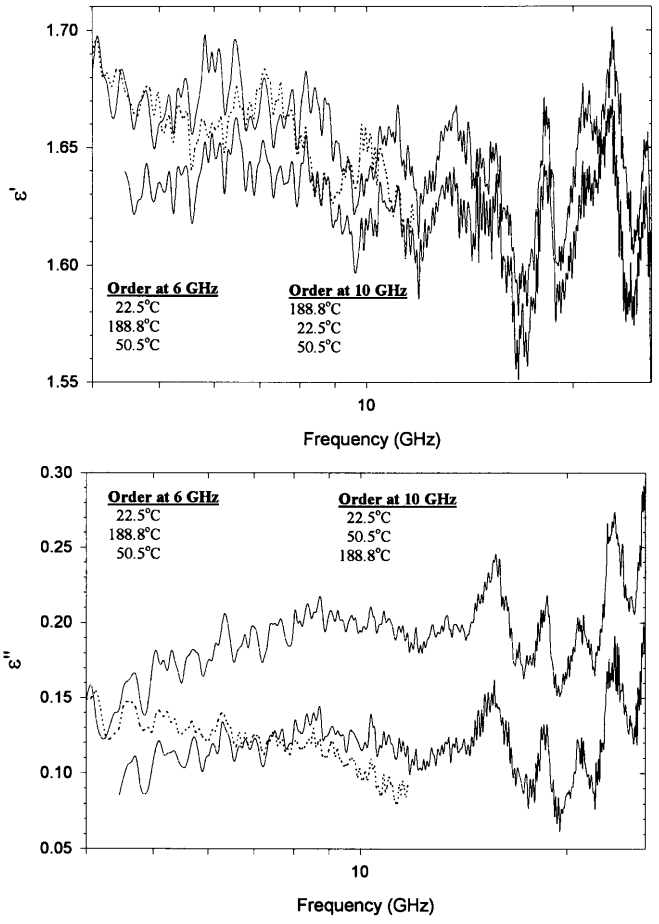

FIGURE 4 Silver oxide: real (ε') and imaginary (ε'') components of complex permittivity

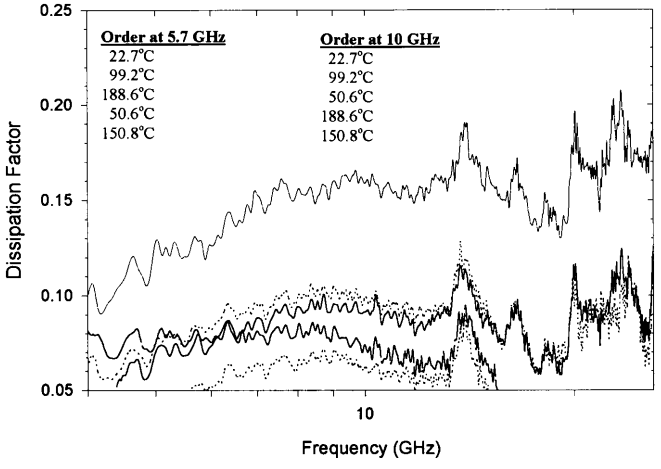

FIGURE 5 Silver carbonate dissipation factor versus frequency

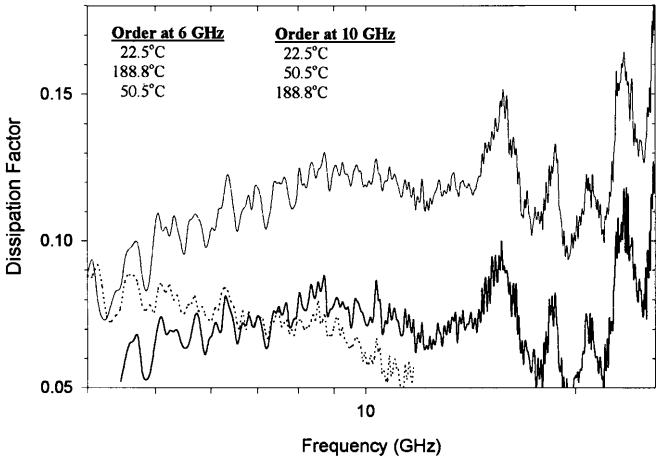

FIGURE 6 Silver oxide dissipation factor versus frequency

For silver carbonate, the real relative permittivity component, which indicates the degree of polarization within the sample, ranges between 1.9 and 2.5. For a given temperature, ε' decreases slightly with increasing frequency. For the two highest temperatures (150.8 °C and 188.6 °C), data are limited to the ranges of 5.6–15.0 GHz and 4–15.6 GHz, respectively. No clear temperature trend is evident. The maximum ε' values occur consistently at the lowest-temperature point (22.7 °C), while the lowest values result from the highest-temperature run (188.6 °C). However, for temperatures between these extrema, the picture is less clear. The deviations with temperature for all data acquired between 22.7 °C and 150.8 °C are relatively small. Also, the frequency response from 50.6 °C appears out of order in the sequence, which generally decreases with increasing temperature. The dielectric loss factors (ε'') for this material range between 0.1 and 0.5. Clear temperature trends are also not evident for the imaginary term. Values of ε'' are greatest at 22.7 °C and least at 150.8 °C. Dissipation factors ($\tan\delta$) range from 0.05 to 0.21, with the highest values occurring consistently across the full spectrum at 22.7 °C.

For silver oxide, only the data acquired at 22.5 °C, 50.5 °C, and 188.8 °C met the $\tan\delta \geq 0.05$ requirement (Fig. 4). For the highest-temperature set point, this requirement was also violated at frequencies above 11.7 GHz. Values of ε' are consistently lower than for silver carbonate, ranging from 1.56 to 1.70. The temperature trends for ε' vary with frequency. For example, at 6 GHz, ε' values decrease according to the series 22.5 °C > 188.8 °C > 50.5 °C, while at 10 GHz the order followed is 188.8 °C > 22.5 °C > 50.5 °C. Dielectric loss factors (ε'') for silver oxide are also consistently lower than for silver carbonate. The temperature dependence of ε'' also varies with frequency. Values of $\tan\delta$ range from 0.05 to 0.18, with maximum values occurring at 22.5 °C and at the 26-GHz high-frequency limit of these experiments.

4 Conclusions

In susceptible solids, heat is produced via oscillating induced interfacial (Maxwell–Wagner) and space-charge polarizations [9–12]. Polarization-relaxation phenomena have been described by Debye as

$$\varepsilon^*(\omega) = \varepsilon_\infty + \frac{\varepsilon_s - \varepsilon_\infty}{1 + i\omega\tau}\,, \tag{9}$$

where ε_s is the static (zero-frequency) permittivity and τ represents the polarization-relaxation time, which is the inverse of the frequency of maximum dielectric loss [13]. The real and imaginary components of the complex permittivity are then described as

$$\varepsilon'(\omega) = \varepsilon_\infty + \frac{\varepsilon_s - \varepsilon_\infty}{1 + (\omega\tau)^2}\,, \tag{10}$$

$$\varepsilon''(\omega) = \frac{\varepsilon_s - \varepsilon_\infty}{1 + (\omega\tau)^2}\omega\tau\,. \tag{11}$$

Slightly more complex representations have been formulated by Cole and Cole [14] and Davidson and Cole [15]. These models require that a plot of ε'' versus ε' in the complex plane will form a semi-circle centered at

$$\varepsilon'(\omega) = \frac{\varepsilon_s + \varepsilon_\infty}{2}\,, \tag{12}$$

where ε_s and ε_∞ represent the permittivity at the low- and high-frequency limits, respectively. These conditions however do not apply with respect to the experimental results for either silver carbonate or silver oxide. Plots of ε'' versus ε' for these materials yield shotgun scatter patterns rather than the semi-circular symmetry imposed by (1) and (2). This is probably due to the relatively low levels of polarization and dielectric loss evident for these two materials under all experimental conditions. From these data it can be concluded that the Ag_2O-Ag_2CO_3 system for the chemisorption of carbon dioxide is not amenable to thermal regeneration via microwave dielectric heating.

ACKNOWLEDGEMENTS This work was funded by the Ames Research Center of the National Aeronautics and Space Administration under Contract No. NAS2-97017. The author thanks Dr. Bernadette K. Luna for her support of this project.

REFERENCES

1 G.V. Colombo, E.S. Mills: Chem. Eng. Prog. Symp. Ser. **62**, 89 (1966)
2 M.S. Nacheff, C.H. Chang, G.V. Colombo, R.J. Cusick: SAE Tech. Pap. Ser. No. 891 595 (1989)
3 J.E. Atwater, J.T. Holtsnider, R.R. Wheeler, Jr.: *Microwave Regenerable Air Purification Device* (National Technical Information Service, Springfield, Virginia 1996)
4 A. von Hippel: *Dielectrics and Waves* (Wiley, New York 1954)
5 A. von Hippel (Ed.): *Dielectric Materials and Applications* (MIT Press, Cambridge, MA 1954)
6 A.K. Jonscher: *Dielectric Relaxation in Solids* (Chelsea Dielectrics Press, London 1983)
7 A.C. Metaxas, R.J. Meridith: *Industrial Microwave Heating* (Peter Perigrinus, London 1983)
8 F. Wang, R. Pottel, U. Kaatze: J. Phys. Chem. B **101**, 922 (1997)
9 C.J.F. Bottcher: *Theory of Electric Polarization* (Elsevier, New York 1952)
10 S. Havriliak, Jr., S.J. Havriliak: *Dielectric and Mechanical Relaxation in Materials* (Hanser, New York 1997)
11 V.I. Gaiduk: *Dielectric Relaxation and Dynamics of Polar Molecules* (World Scientific, New Jersey 1999)
12 A.K. Jonscher: J. Phys. D: Appl. Phys. **32**, R57 (1999)
13 P. Debye: *Polar Molecules* (Lancaster Press, Lancaster, PA 1929)
14 K.S. Cole, R.H. Cole: J. Chem. Phys. **9**, 341 (1941)
15 D.W. Davidson, R.H. Cole: J. Chem. Phys. **19**, 1484 (1951)